FORMATION OF HYDRAULIC JUMPS ON CORRUGATED BEDS

Ibrahim H. Elsebaie[1] and Shazy Shabayek[2]

***Abstract*— A study of the effect of different shapes of corrugated beds on the characteristics of hydraulic jumps was conducted. Experiments were performed for a range of the Froude number from 3 to 7.5. Five shapes of corrugations (sinusoidal, triangular, trapezoidal with two side slopes and rectangular) of the same amplitude and wavelength were tested. Two values of relative roughness t/y_1 of 0.36 and 0.72 were studied. It was found that, for all shapes of corrugated beds, the tailwater depth required to form a jump was appreciably smaller than that for the corresponding jumps on smooth beds. Further, the length of the jump on the different corrugated beds was less than half of that on smooth beds. The integrated bed shear stress on the corrugated beds was more than 15 times that on smooth beds. For the same amplitude and wavelength, it was found that the effect of the shape of corrugations is relatively small. The results of this study confirm the effectiveness of corrugated beds for energy dissipation below hydraulic structures.**

KEYWORDS*: *Corrugated Beds,* Energy *dissipation,, Hydraulic jump, Open channel flow.

1. INTRODUCTION

Hydraulic jumps have been widely used for energy dissipation below hydraulic structures. In hydraulic-jump-type energy dissipators, the jumps are often formed with the assistance of baffle blocks and are kept inside the stilling basin even when the tailwater depth is somewhat less than the sequent depth of the free jump [1]. A jump formed in a horizontal, wide rectangular channel with a smooth bed is often referred to as the classic hydraulic jump and has been studied extensively [1], [2], [3], and [4]. If y_1 and $U_1$are, respectively, the depth and mean velocity of the supercritical stream just upstream of the jump, with a Froude number of $F_1=U_1/(gy_1)^{0.5}$ where g is the acceleration due to gravity, the subcritical sequent depth y_2^* is given by the well- known Belanger equation

$$y_2^*/y_1 = 1/2[\sqrt{1+8F_1^2} - 1] \qquad (1)$$

A preliminary investigation by [5] indicated that, if the bed of the channel on which the jump is formed is rough, the tailwater depth y_2 required to form a jump could be appreciably smaller than the corresponding sequent depth y_2^*. For a relative roughness of the bed in terms of the supercritical depth y_1 equal to about 0.4, y_2 could be as small as $0.8y_2^*$, which is significant when it is realized that the tailwater depth required for Peterka's Basins II and III in terms of y_2^* are approximately 0.83 and 0.97, respectively. Further studies by [6], [7] and others (see [4]) have supported this reduction in the required tailwater depth produced by the roughness of the bed. Further, [5] found that the jumps on rough beds were significantly shorter than the classical jump.

Reference [8] performed a laboratory study of hydraulic jumps on corrugated beds for a range of Froude numbers from 4 to 10 and three values of the relative roughness t/y_1 from 0.25 to 0.50. Reference [8] found that the ratio y_2/y_1 of the tailwater depth to the supercritical depth needed to form a jump for any Froude number was noticeably smaller than that for the corresponding jump on a smooth bed. Reference [8] explained that the reason for the reduction of the jump–forming tailwater depth appeared to be the enhanced bed shear stresses produced by the interaction of the supercritical stream with the bed corrugations. Reference [8] added that the bed shear stress on corrugated beds was about ten times that on smooth beds. Reference [9] conducted an experimental study to investigate the effect of trapezoidal shaped corrugated beds on the characteristics of hydraulic jump. They confirmed the results of reference [8]. Reference [9] added that the jump length is more dependent on the wave length of corrugations than their amplitude.

2. EXPRIMENTAL SETUP AND PROCEDURE

A. Hydraulic jumps were produced in a Rectangular flume 29.5 cm wide, 32.0 cm deep and 9.0 m long. The side walls of the flume were made of transparent Plexiglas sheets. Water was pumped from a storage tank to the head tank of the flume by a centrifugal pump. Corrugated plastic sinusoidal sheets and corrugated wooden triangular, rectangular and trapezoidal sheets (see Fig. 1(a-e)) were installed on the flume bed in such a way that the crests of corrugations were at the same level as the upstream bed on which the supercritical stream was produced by a sluice gate. The corrugations acted

Manuscript received January 8, 2010.

[1]Assistant Professor, Civil Engineering Department, King Saud University, Riyadh, KSA; phone: 00966501214635; fax: 0096614677008; e-mail: elsebaie@ksu.edu.sa

[2]Associate Professor, Department of Civil Engineering, Ain Shams University, Cairo, Egypt; e-mail: Shazy@ualberta.net

as depressions in the bed, to create a system of turbulent eddies which might increase the bed shear stresses. All the five types of corrugations (I, II, III, IV and V) had a wavelength s of 65 mm in the flow direction and an amplitude t of 18 mm. One of the two trapezoidal sections and the triangular section had side slopes of 45 degrees. The other trapezoidal section had side slopes of 60 degrees. The discharges were measured by a V-notch installed in a measuring tank located at the end of the flume. Water entered the flume under a sluice gate with a streamlined lip, thereby producing a uniform supercritical stream with a thickness of y_1*. A tailgate was used to control the tailwater depth in the flume. In all the experiments, the tailgate was adjusted so that the jumps were formed on the corrugated beds (see Fig. 2).*

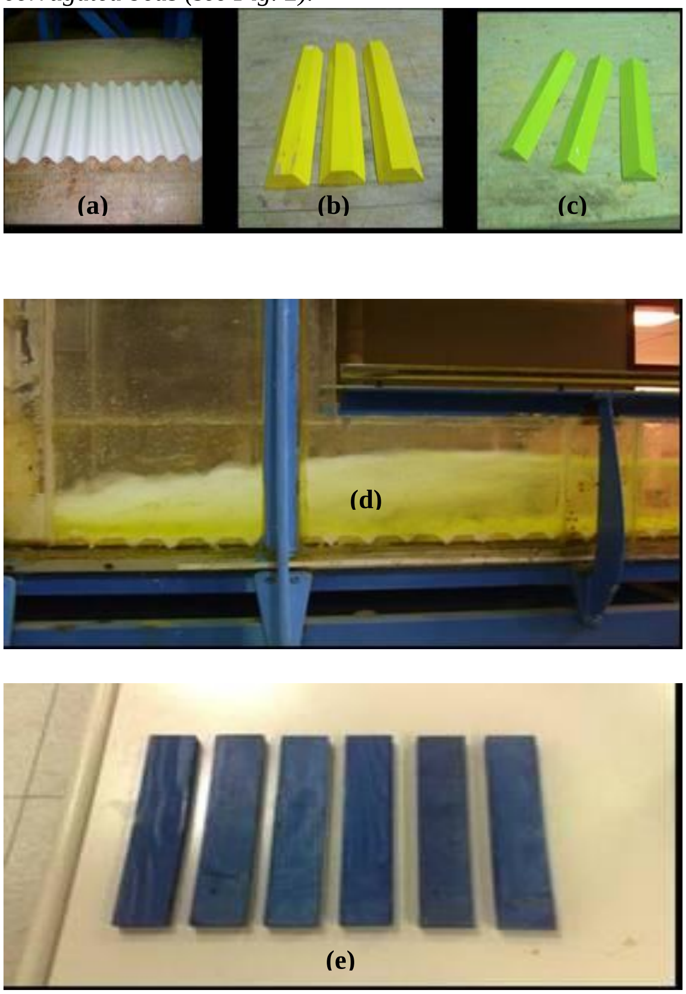

Fig. 1 (a) Sinusoidal; (b) Trapezoidal (45^o side slopes); (c) Triangular; (d) Trapezoidal (60^o side slopes); and (e) Rectangular Corrugations

A total of 55 experiments (11 for every sheet) were conducted and the primary details of these experiments are shown in table 1. For all the five sheets six experiments of series A and five experiments of series B were conducted. The initial depth y_1, measured above the crest level of corrugations on the plane bed, was equal to 25 mm in the A series and 50 mm in the B series. Values of y_1 and V_1 were selected to achieve a wide range of the Froude number, from 3 to 7.5. The Reynolds number $R_1=V_1y_1/\upsilon$ was in the range of 49,523-142,157. Two values of the relative roughness, defined as the ratio of the amplitude of the corrugations to the supercritical depth just before the jump, t/y_1 of 0.36 and 0.72 were investigated.

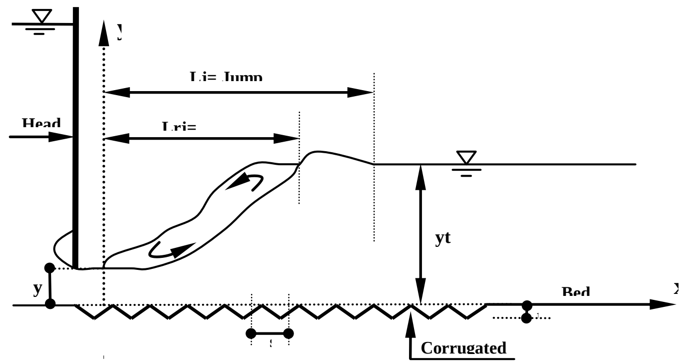

Fig. 2 Definition sketch for free jumps on corrugated beds (sheet II)

3. EXPERIMENTAL RESULTS AND ANALYSIS

3.1 WATER SURFACE PROF*ILES*

Figs. 3(a-e) show the water surface profiles for the A series experiments of the jumps on the five corrugated sheets, respectively. These profiles were measured in the vertical centerplane of the flume with, a point gauge to an accuracy of 0.1 mm. These water surface profiles were used to determine the subcritical sequent depth y_2 at the end of the jump, which was defined as the section beyond which the water surface was essentially horizontal, and the length of the jump L_j. Normalized water surface profiles are shown in Figs. 4(a-e) where $(y-y_1)/(y_2-y_1)$ is plotted against x/L_j, with y the depth of flow at any station x. Figs. 4(a-e) show that the water surface profiles, for each type of corrugated beds, are approximately similar and can be represented by one mean curve.

3.2 SEQUENT DEPTH RATIO

For a jump on a corrugated bed of corrugation amplitude t, with a supercritical stream of depth y_1 and mean velocity V_1, the depth at the end of the jump y_2 may be written as

$$y_2 = f_1(y_1, U_1, g, \rho, \upsilon, t, \xi) \qquad (2)$$

Where ρ = mass density and ν = kinematic viscosity of the fluid, ξ represents the shape of the corrugated bed. Using the Pi theorem, it can be shown that

$$y_2/y_1 = f_2\left(F_1=U_1/(gy_1)^{0.5},\ R_1= U_1y_1/\upsilon,\ t/y_1,\ \xi\right) \qquad (3)$$

For large values of the Reynolds number (involved in this study), viscous effects may be neglected (see [10] and [11]) and (3) reduces to

$$y_2/y_1 = f_3 (F_1, t/y_1, \xi) \quad (4)$$

The experimental results are shown in Fig. 5 with y_2/y_1 plotted against F_1 for series A (t/y_1 = 0.72) and series B (t/y_1 = 0.36) for the five types of corrugated beds. Eq. 1 (Belanger Equation) is also shown in Fig. 5. It can be seen from Fig. 5 that the relative roughness and shape of corrugations do not have significant effects on the depth ratio. It was also found that the depth ratio y_2/y_1 is approximately equal to 88% of the supercritical Froude number F_1. Hence, (4) could be written as

$$y_2/y_1 = 0.88F_1 \quad (r^2=0.94) \quad (5)$$

Since the corrugations were set with their crests at the upstream bed level, the corrugation acted like cavities and the t/y_1, values were not important. In the experiments conducted by [5], with protruding roughness elements, the relative roughness height was an important parameter. For relatively large values of the Froude number F_1, the sequent depth ratio for the classical jump can be written as

$$\frac{y_2^*}{y_2} = \sqrt{2}F_1 - 1 = \sqrt{2}F_1 \quad (6)$$

To get an appreciation for the reduction in the tailwater depth y_2 required to form a jump on a corrugated bed in comparison with y_{2*} of the corresponding classical jump, let us define a dimensionless depth deficit parameter D = (y_2*-y_2)/y_2*. It may be observed that this parameter is similar to the submergence factor of submerged hydraulic jumps [2]. Fig. 6 shows the variation of D with F_1 for all the experiments (series A and series B) for the five shapes of corrugated beds used in the experiments (i.e. sinusoidal, triangular, two trapezoidal and rectangular) and the results indicate a constant value of approximately 0.37. A value of 0.25 was found by [8]. Also, using (5) and (6), it can be shown that $D = (\sqrt{2} - 0.88)/\sqrt{2} \cong 0.38$. This means that corrugated beds are very efficient in the formation of hydraulic jumps, compared to some of the stilling basins (especially Types II and III) developed by [1]. Also, these results confirm that the shape of corrugations and their relative height (t/y_1) do not play an important role in the hydraulic jump characteristics.

3.3 JUMP LENGTH

It was shown earlier that the sequent depth of the jump on corrugated beds y_2 is appreciably shallower than that of jumps on smooth beds. It is understood, from the momentum balance, that the increased bed shear stress is responsible for the decreased sequent depth of jumps on corrugated beds. If F_τ is the integrated bed shear stress on the horizontal plane coinciding with the crests of the corrugations along the length of the jump, it can be found using the integral momentum equation that

$$F_\tau = (P_1 - P_2) + (M_1 - M_2) \quad (7)$$

Where P_1, P_2 and M_1, M_2 are the integrated pressures and momentum fluxes at the sections just at the beginning and end of the jump. Using the relation $F_\tau = \varepsilon_1 M_1$ and following [12], (7) can be reduced to the form

$$(y_2/y_1)^3 - (1 + 2F_1^2 - 2\varepsilon_1 F_1^2)(y_2/y_1) + 2F_1^2 = 0 \quad (8)$$

Equation (8) reduces to the Belanger equation when the shear force on the bed is neglected.

Substituting (5) in (8), we obtain

$$\varepsilon_1 = (1.23F_1^2 - 2.27F_1 + 1) / 2F_1^2 \quad (9)$$

The shear force coefficient introduced by [13] was defined as

$\varepsilon = F_\tau / \gamma y_1^2 / 2$. It can be shown, for the range of the Froude number used in this study, that

$$\varepsilon = 2\varepsilon_1 F_1^2 = 1.23F_1^2 - 2.27F_1 + 1 \quad (10)$$

The equation for the shear stress coefficient for jumps on smooth beds may be written as

$$\varepsilon = 0.16 F_1^2 - 0.80 F_1 + 1.00 \quad (11)$$

Figure 8 shows the variation of shear force coefficient ε with the supercritical Froude number F_1 for jumps on corrugated beds for the all shapes of corrugations used in this study along with the mean curve for jumps formed on smooth beds [13]. Also, included in Figure 8 are the results of [8]. A number of interesting observations could be made from a study of Fig. 8. First, the data for the corrugated beds used in the present study can be represented by one mean curve. This confirms that the bed shear stress on corrugated beds is independent of the shape of corrugations. Second, the trend of the relationship between ε and F_1 is the same for smooth and corrugated beds for the present study and those of [8], [9] and [14]. Third, although the trend of the relation between ε and F_1 is similar, there are considerable differences among the shear stress values for the present study and those of [8], [9] and [14]. For a supercritical Froude number F_1 equal to 5, the value of ε for smooth beds is 1 and the values of ε for corrugated beds for the present study and those of [8], [9] and [14] are 20, 16, 8, and 22, respectively. It seems that the dynamics of the boundary shear stress on corrugated beds and the factors affecting it are not completely understood and need further investigation so that these discrepancies would be properly explained.

4. CONCLUSION

Based on a laboratory study of hydraulic jumps on Sinusoidal, Trapezoidal (45^o side slopes), Triangular, Trapezoidal (60^o side slopes) and Rectangular corrugated beds for a range of the Froude number from 3 to 7.5 and two values of the relative roughness t/y_1 of 0.36 and 0.72, the following conclusions could be made. Normalized water surface profiles for each individual corrugated sheet for the larger value of the relative roughness (t/y_1=0.72) could be represented by one mean curve. The ratio y_2/y_1 of the tailwater depth to the supercritical depth needed to form a jump for any Froude number is noticeably smaller than that for the corresponding jump on a smooth bed. This ratio was found to be equal to about 88% of the supercritical Froude number. If D is the dimensionless depth deficit equal to $(y_2^*-y_2)/y_2^*$, for the range of parameters investigated, D was approximately equal to 0.37. The normalized Jump length L_j/y_2^* was found to be equal to 2.1 compared to a value of 3 introduced by [8] for their experiments on jumps on sinusoidal corrugated beds and a value of 2.25 introduced by [14] for their experiments on jumps on sinusoidal, trapezoidal and triangular corrugated beds. It is interesting to know that the normalized jump length for Peterka's Type II basin is about 6.

The reason for the reduction of the jump-forming tailwater depth appears to be the enhanced bed shear stresses produced by the interaction of the supercritical stream with the bed corrugations. The variation of the integrated bed shear stress on the different shapes of corrugated beds was studied. It was found that all the five corrugated beds used in the present study could be represented by one mean curve confirming that the shear stress on corrugated beds is independent of the shape of corrugations. Also, it was found that the trend of the relationship between ε and F_1 is the same for smooth and corrugated beds for the present study and those of [8], [9] and [14]. Although the trend of the relation between ε and F_1 is similar, there are considerable differences among the values of the shear stress for the present study and those of [8], [9] and [14]. It seems that the dynamics of the boundary shear stress on corrugated beds and the factors affecting it are not completely understood and need further investigation so that these differences would be properly explained.

ACKNOWLEDGMENT

The author expresses his sincere gratitude to the Research Center of the Faculty of Engineering, King Saud University for supporting this work.

REFERENCES

[1] A. J. Peterka, "Hydraulic design of stilling basins and energy dissipators" *Engineering Monograph No. 25*, U.S. Bureau of Reclamation, Denver, 1958.

[2] N. Rajaratnam, "Hydraulic jumps." *Adv. Hydrosci.*, 1967, 4, 197–280.

[3] J. A. McCorquodale, "Chapter 8: Hydraulic jumps and internal flows." *Encyclopedia of fluid mechanics*, N. P. Cheremisinoff, ed., Vol. 2, Gulf Publishing, Houston, 1986, 120–173.

[4] W. H. Hager, "*Energy dissipators and hydraulic jump*", Kluwer Academic, Dordrecht, 1992.

[5] N. Rajaratnam, "Hydraulic jumps on rough beds." *Trans. Eng. Inst. Canada*, 1968, 11(A-2), 1–8.

[6] W. C., Hughes, J. E. and Flack, "Hydraulic jump properties over a rough bed." *J. Hydraul. Eng.*, 1984, 110(12), 1755–1771.

[7] S. A., Ead, N., Rajaratnam, C., Katopodis, and F. Ade, "Turbulent open-channel flow in circular corrugated culverts.'" *J. Hydraul. Eng.*, 2000, 126(10), 750–757.

[8] S. A., Ead, and N. Rajaratnam, "Hydraulic jumps on corrugated beds." *Journal of Hydraulic Engineering*, ASCE, 2002a, Vol. 128, No. 7, pp. 656-663.

[9] F., Izadjoo, and M. Shafai-Bajestan, "Effects of Trapezoidal shape corrugated bed on the characteristics of Hydraulic jump." 17th Canadian Hydrotechnical Conference, Hydrotechnical Engineering: Cornerstone of a Sustainable Environment, Edmonton, Alberta, Canada, 2005, August 17–19.

[10] N. Rajaratnam, "*Turbulent jets*, Elsevier Science", Amsterdam, The Netherlands, 1976.

[11] W. H., Hager, and R. Bremen, "Classical hydraulic jump; sequent depths." *J. Hydraul. Res.*, 1989, 27(5), 565–585.

[12] S. A., Ead, and N. Rajaratnam, "Plane turbulent wall jets in shallow tailwater." *J. Eng. Mech.*, 2002b, 128(2), 143–155.

[13] N. Rajaratnam, "The hydraulic jump as a wall jet." *J. Hydraul. Div., Am. Soc. Civ. Eng.*, 1965, 91(5), 107–132.

[14] S. A., Ead, and I. H. Elsebaie "Effect of bed corrugations on the characteristics of a hydraulic jump " *Journal of Faculty of Engineering*, Al-Azhar University, CERM, 2009, Vol. 31, No. 1, pp. 238-251.

Table (1): Primary Details of Experiments

Expt	Sheet	F_1	R_1	U_1 (m/s)	y_1 (mm)	y_2 (m)	y_2* (m)	L_j (m)	D	t/y_1	L_j/y_2*	$F_\tau/\gamma y_1^2/2$
A1	I	4.1	51047	2.04	25	0.075	0.134	0.220	0.439	0.72	1.644	14.667
A2	I	5.0	61903	2.48	25	0.080	0.165	0.250	0.514	0.72	1.518	25.135
A3	I	5.7	71122	2.84	25	0.095	0.191	0.400	0.503	0.72	2.094	35.192
A4	I	6.4	79275	3.17	25	0.136	0.214	0.500	0.365	0.72	2.334	38.333
A5	I	7.0	86488	3.46	25	0.142	0.235	0.600	0.395	0.72	2.555	49.155
A6	I	7.5	93374	3.73	25	0.145	0.254	0.650	0.430	0.72	2.555	61.506
B1	I	3.0	105054	2.10	50	0.124	0.189	0.220	0.343	0.36	1.166	5.592
B2	I	3.3	116141	2.32	50	0.134	0.211	0.350	0.364	0.36	1.660	7.609
B3	I	3.6	126259	2.53	50	0.146	0.231	0.400	0.368	0.36	1.730	9.569
B4	I	3.9	135624	2.71	50	0.150	0.250	0.430	0.400	0.36	1.720	12.000
B5	I	4.1	142157	2.84	50	0.154	0.263	0.450	0.415	0.36	1.710	13.772
A1	II	4.1	51047	2.04	25	0.060	0.134	0.170	0.552	0.72	1.270	15.073
A2	II	5.0	61903	2.48	25	0.092	0.165	0.230	0.441	0.72	1.396	23.871
A3	II	5.7	71122	2.84	25	0.105	0.191	0.350	0.450	0.72	1.833	33.646
A4	II	6.4	79275	3.17	25	0.121	0.214	0.400	0.435	0.72	1.867	42.632
A5	II	7.0	86488	3.46	25	0.141	0.235	0.430	0.399	0.72	1.831	49.485
A6	II	7.5	93374	3.73	25	0.147	0.254	0.500	0.422	0.72	1.965	60.839
B1	II	3.0	105054	2.10	50	0.110	0.189	0.200	0.417	0.36	1.060	5.978
B2	II	3.3	116141	2.32	50	0.115	0.211	0.300	0.455	0.36	1.423	8.145
B3	II	3.6	126259	2.53	50	0.120	0.231	0.330	0.481	0.36	1.427	10.407
B4	II	3.9	135624	2.71	50	0.133	0.250	0.350	0.468	0.36	1.400	12.646
B5	II	4.1	142157	2.84	50	0.155	0.263	0.400	0.411	0.36	1.520	13.718
A1	III	4.1	51047	2.04	25	0.075	0.134	0.200	0.439	0.72	1.495	14.667
A2	III	5.0	61903	2.48	25	0.100	0.165	0.310	0.393	0.72	1.882	22.500
A3	III	5.7	71122	2.84	25	0.120	0.191	0.470	0.372	0.72	2.461	30.210
A4	III	6.4	79275	3.17	25	0.125	0.214	0.520	0.417	0.72	2.427	41.600
A5	III	7.0	86488	3.46	25	0.150	0.235	0.550	0.361	0.72	2.342	46.333
A6	III	7.5	93374	3.73	25	0.160	0.254	0.650	0.371	0.72	2.555	56.025
B1	III	3.0	105054	2.10	50	0.115	0.189	0.220	0.390	0.36	1.166	5.884
B2	III	3.3	116141	2.32	50	0.130	0.211	0.420	0.383	0.36	1.992	7.778
B3	III	3.6	126259	2.53	50	0.145	0.231	0.530	0.373	0.36	2.293	9.624
B4	III	3.9	135624	2.71	50	0.155	0.250	0.570	0.380	0.36	2.280	11.713
B5	III	4.1	142157	2.84	50	0.165	0.263	0.620	0.373	0.36	2.356	13.082

A1	IV	4.1	51047	2.04	25	0.104	0.134	0.515	0.223	0.72	3.849	9.977
A2	IV	5.0	61903	2.48	25	0.123	0.165	0.545	0.253	0.72	3.309	17.621
A3	IV	5.7	71122	2.84	25	0.140	0.191	0.605	0.267	0.72	3.168	24.809
A4	IV	6.4	79275	3.17	25	0.160	0.214	0.870	0.253	0.72	4.061	30.431
A5	IV	7.0	86488	3.46	25	0.170	0.235	1.070	0.276	0.72	4.557	39.788
A6	IV	7.5	93374	3.73	25	0.180	0.254	1.200	0.293	0.72	4.716	48.644
B1	IV	3.0	105054	2.10	50	0.150	0.189	0.550	0.205	0.36	2.916	6.551
B2	IV	3.3	116141	2.32	50	0.160	0.211	0.624	0.241	0.36	2.959	8.047
B3	IV	3.6	126259	2.53	50	0.168	0.231	0.760	0.273	0.36	3.288	9.545
B4	IV	3.9	135624	2.71	50	0.176	0.250	0.900	0.296	0.36	3.600	10.959
B5	IV	4.1	142157	2.84	50	0.180	0.263	1.100	0.316	0.36	4.180	13.525
A1	V	4.1	51047	2.04	25	0.080	0.134	0.355	0.402	0.72	2.653	16.234
A2	V	5.0	61903	2.48	25	0.100	0.165	0.420	0.393	0.72	2.550	25.178
A3	V	5.7	71122	2.84	25	0.120	0.191	0.570	0.372	0.72	2.985	32.889
A4	V	6.4	79275	3.17	25	0.138	0.214	0.780	0.356	0.72	3.641	39.717
A5	V	7.0	86488	3.46	25	0.150	0.235	1.000	0.361	0.72	4.259	49.264
A6	V	7.5	93374	3.73	25	0.163	0.254	1.140	0.359	0.72	4.480	57.411
B1	V	3.0	105054	2.10	50	0.137	0.189	0.584	0.274	0.36	3.096	5.943
B2	V	3.3	116141	2.32	50	0.149	0.211	0.782	0.293	0.36	3.709	8.194
B3	V	3.6	126259	2.53	50	0.157	0.231	0.913	0.321	0.36	3.949	10.116
B4	V	3.9	135624	2.71	50	0.165	0.250	1.070	0.340	0.36	4.280	12.157
B5	V	4.1	142157	2.84	50	0.188	0.263	1.180	0.286	0.36	4.484	12.992

Sheet I : Sinusoidal Corrugated Bed

Sheet II : Triangular Corrugated Bed

Sheet III : Trapezoidal (45^o side slopes) Corrugated Bed

Sheet IV : Trapezoidal (60^o side slopes) Corrugated Bed

Sheet V : Rectangular Corrugated Bed

t : Corrugation height (from crest to trough) = 18 mm

s : Corrugation Wavelength = 65 mm

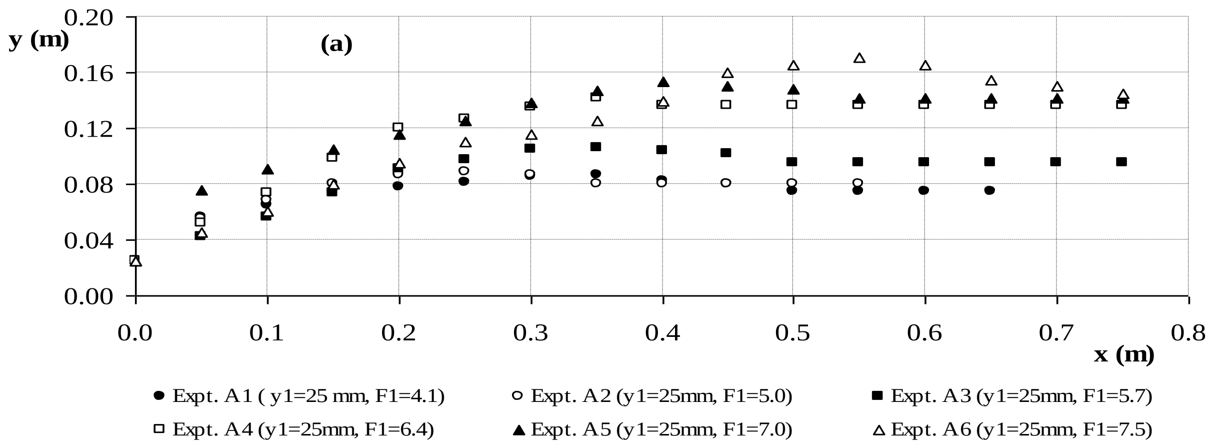
y (m)
(a)
0.20
0.16
0.12
0.08
0.04
0.00
0.0
0.1
0.2
0.3
0.4
0.5
0.6
0.7
0.8
x (m)
Expt. A1 (y1=25 mm, F1=4.1)
Expt. A2 (y1=25mm, F1=5.0)
Expt. A3 (y1=25mm, F1=5.7)
Expt. A4 (y1=25mm, F1=6.4)
Expt. A5 (y1=25mm, F1=7.0)
Expt. A6 (y1=25mm, F1=7.5)

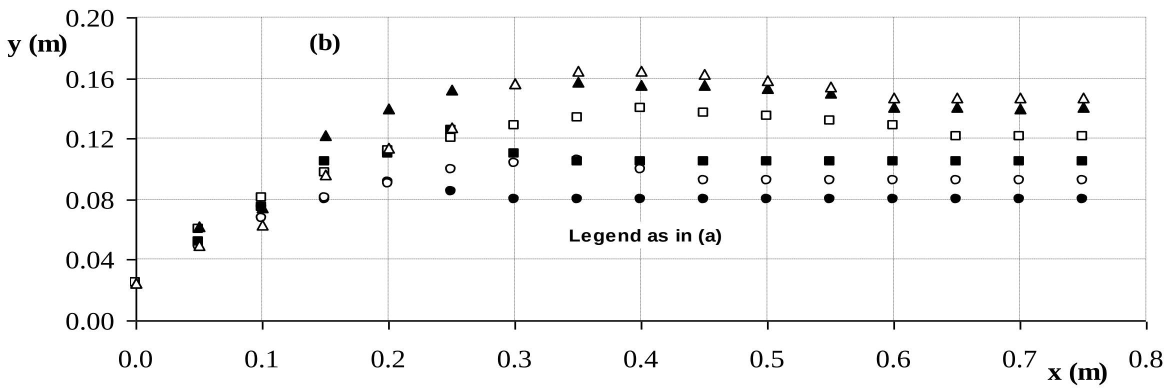
y (m)
(b)
0.20
0.16
0.12
0.08
0.04
0.00
Legend as in (a)
0.0
0.1
0.2
0.3
0.4
0.5
0.6
0.7
0.8
x (m)

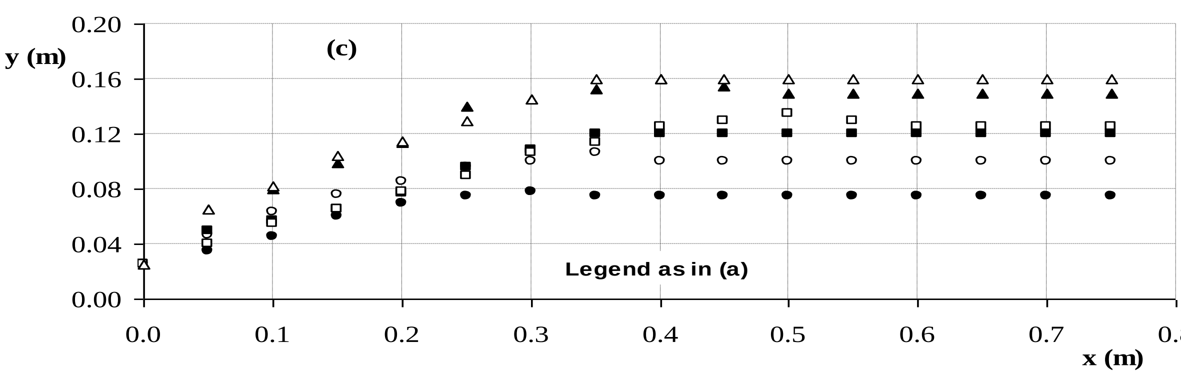
y (m)
(c)
0.20
0.16
0.12
0.08
0.04
0.00
Legend as in (a)
0.0
0.1
0.2
0.3
0.4
0.5
0.6
0.7
0.8
x (m)

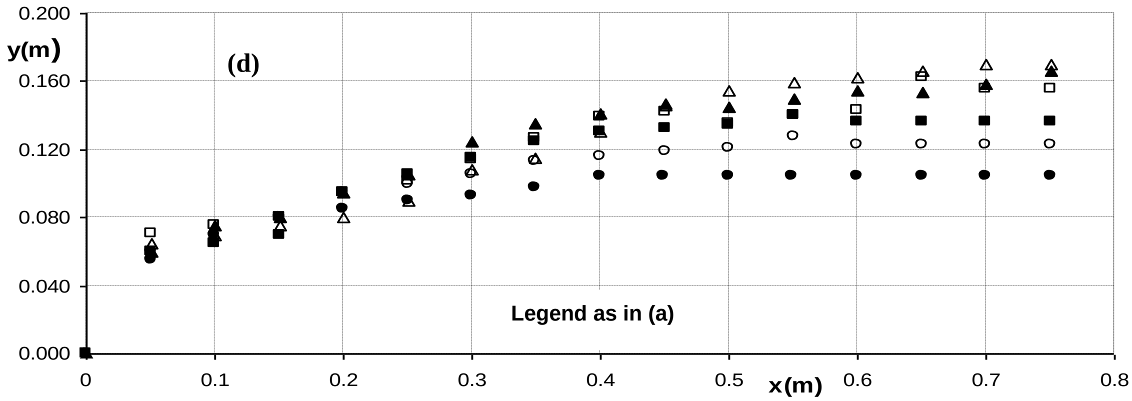

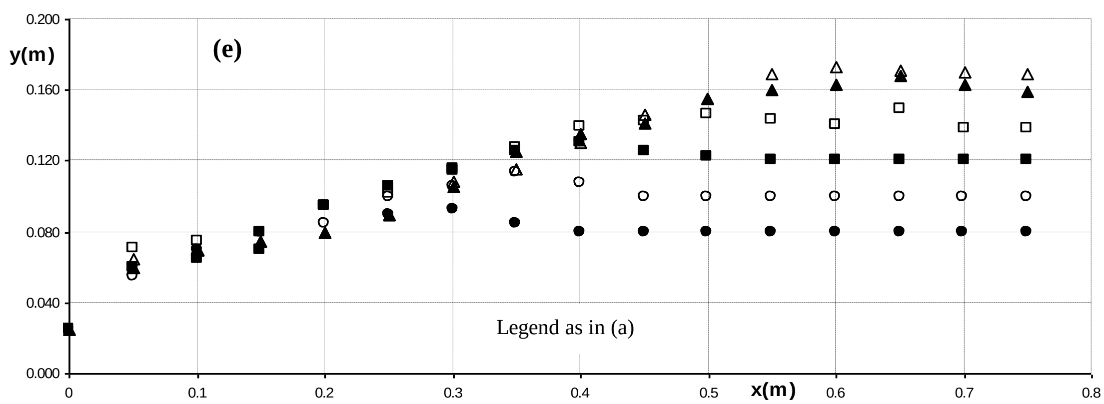

Fig. 3(a-e) Water surface profiles for the (A) series experiments for jumps on (a) Sinusoidal; (b) Trapezoidal (45° side slopes); (c) Triangular; (d) Trapezoidal (60° side slopes); and (e) Rectangular Corrugated beds, respectively

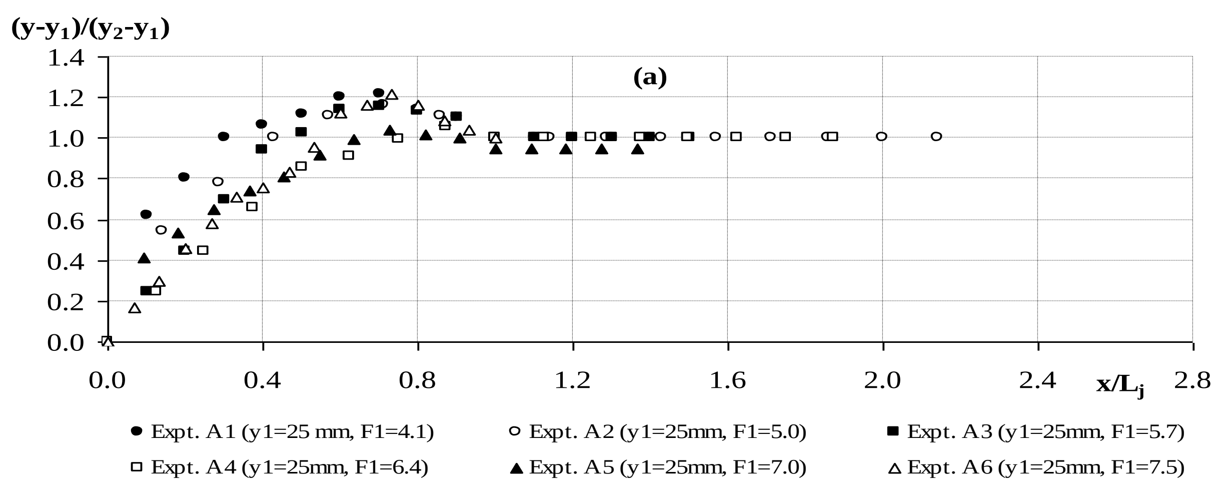

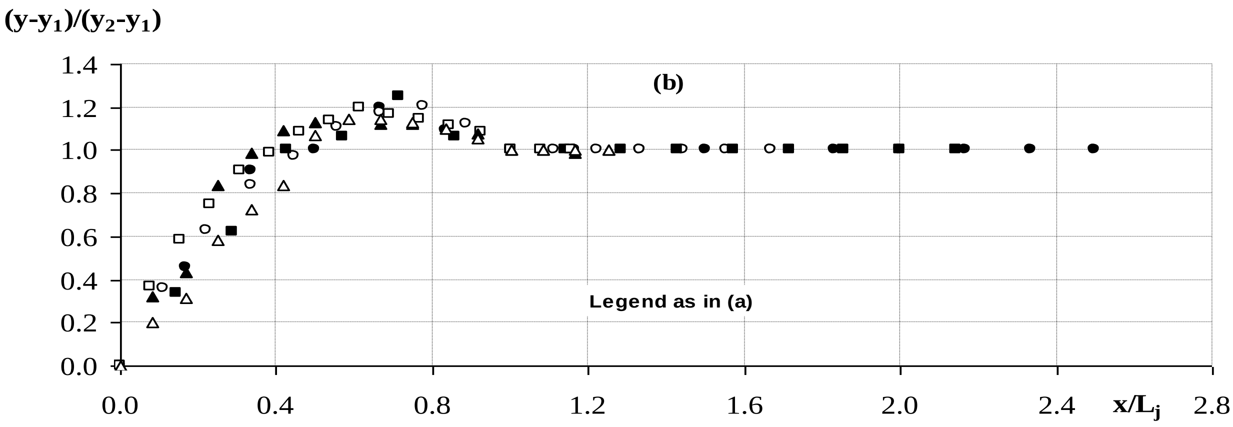
$(y-y_1)/(y_2-y_1)$
(b)
Legend as in (a)
x/L_j

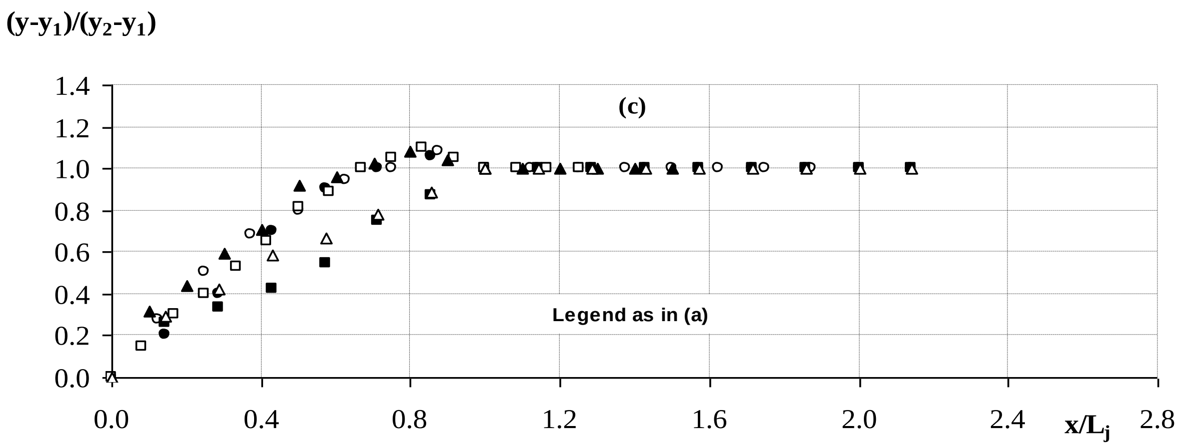
$(y-y_1)/(y_2-y_1)$
(c)
Legend as in (a)
x/L_j

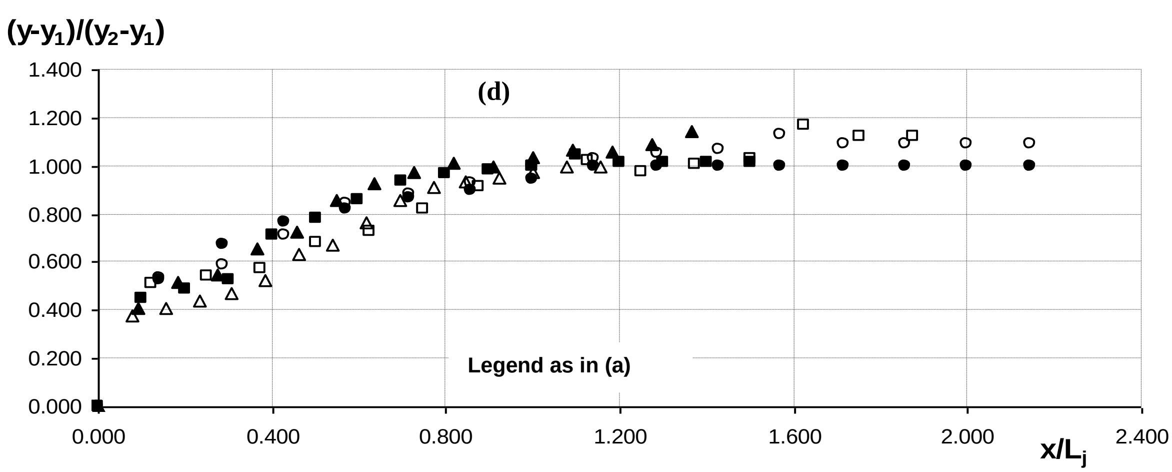
$(y-y_1)/(y_2-y_1)$
(d)
Legend as in (a)
x/L_j

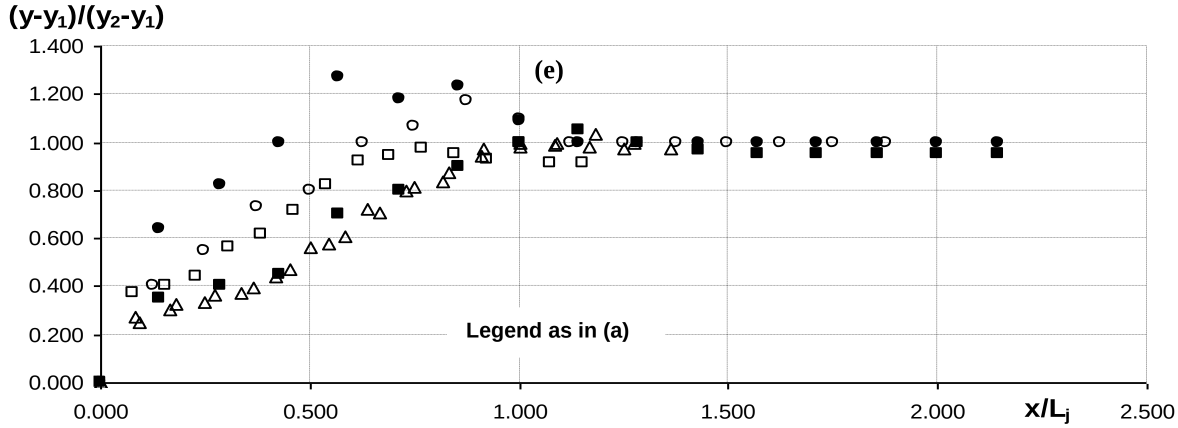

Fig. 4(a-e) Normalized Water surface profiles for the (A) series experiments for jumps on (a) Sinusoidal; (b) Trapezoidal (45^o side slopes); (c) Triangular; (d) Trapezoidal (60^o side slopes); and (e) Rectangular Corrugated beds, respectively

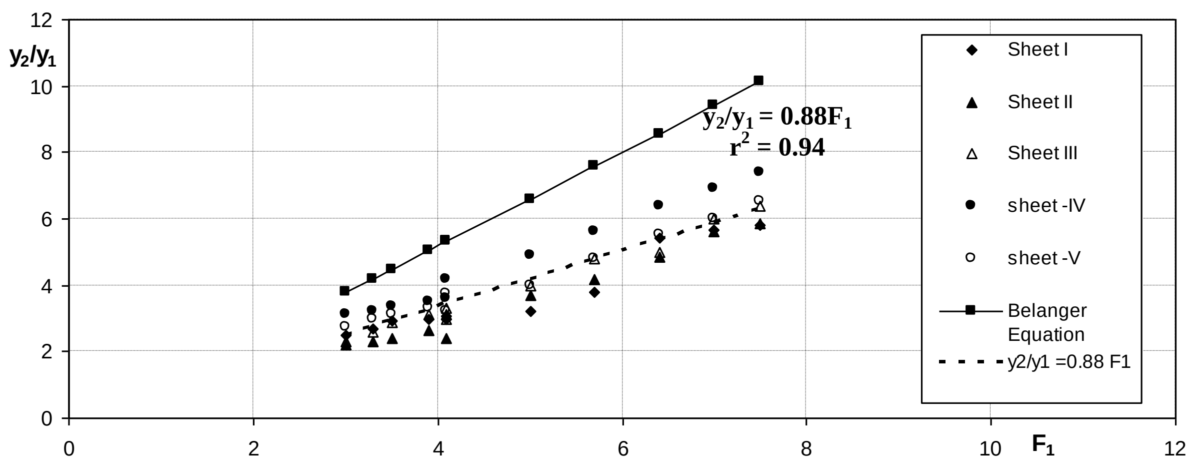

Fig.5 Variation of the sequent depth ratio (y_2/y_1) with the Froude number F_1 for all Experiments

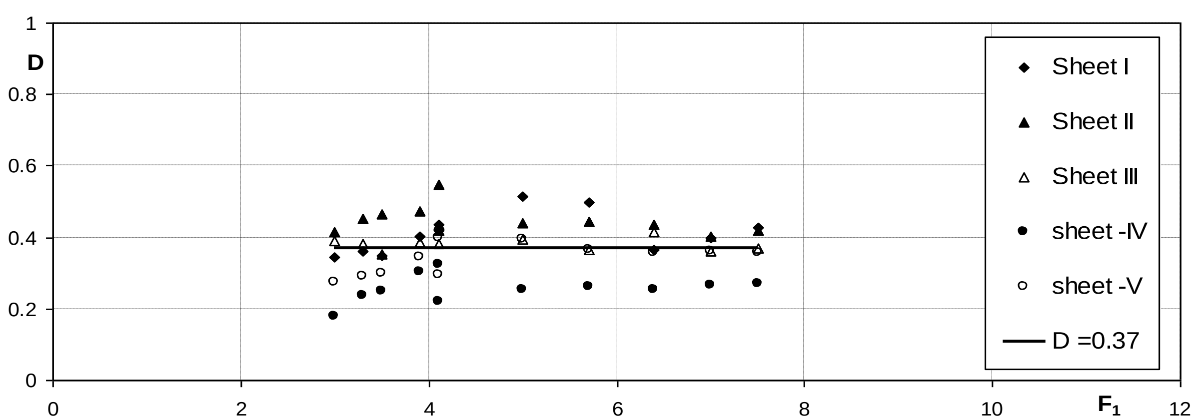

Fig.6 Variation of the depth deficit factor ($D= (y_2^*-y_2)/y_2^*$) with the Froude number F_1 for all Experiments

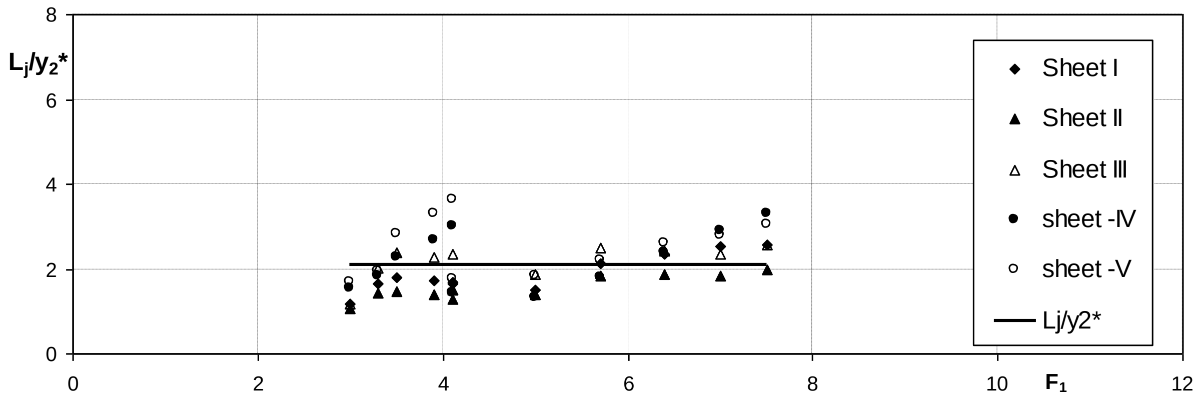

Fig.7 Variation of the normalized jump length (L_j/y_2^*) with the Froude number F_1 for all Experiments

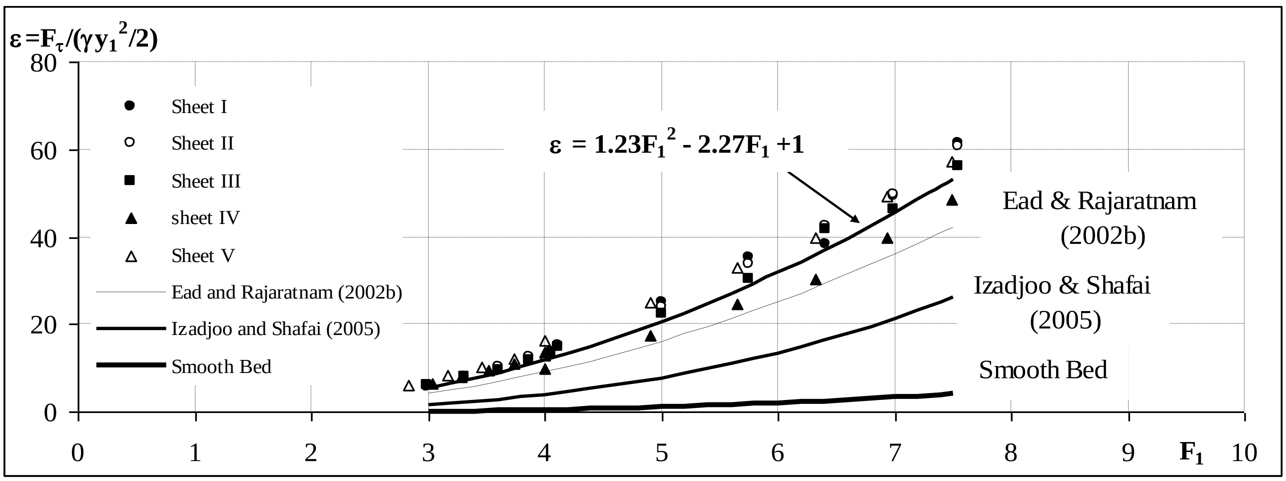

Fig.8 Variation of the Shear Force Coefficient ε with the Froude Number F_1